Surfactant double layer stabilized magnetic nanofluids for biomedical application

2008 J. Phys.: Condens. Matter 20 204103

(http://iopscience.iop.org/0953-8984/20/20/204103)

J. Phys.: Condens. Matter **20** (2008) 204103 (6pp) doi:10.1088/0953-8984/20/20/204103

Surfactant double layer stabilized magnetic nanofluids for biomedical application

E Tombácz[1], D Bica[2], A Hajdú[1], E Illés[1], A Majzik[1] and L Vékás[2]

[1] Department of Colloid Chemistry, University of Szeged, Hungary
[2] Center of Fundamental and Advanced Technical Research, Romanian Academy-Timisoara Division, Romania

E-mail: tombacz@chem.u-szeged.hu

Received 1 April 2008
Published 1 May 2008
Online at stacks.iop.org/JPhysCM/20/204103

Abstract

Magnetite nanoparticles were coated with surfactant double layers in order to prepare water based magnetic fluids (MFs). The effects of head group (sulfonate, carboxylate) and alkyl chain length (11–17 C atoms) and the combination of surfactants were studied. Adsorption, dynamic light scattering (DLS) and electrophoretic mobility measurements were performed. The quantity of surfactant varied between 0.3 and 0.5 g, i.e. their specific amount ranges over 1.5–2 mmol g^{-1} magnetite in MFs. The adsorption isotherm of Na oleate on magnetite proved the double layer formation with 2 mmol g^{-1} saturation value in good harmony with the empirical doses. The effect of diluting MFs, pH and salt concentration was studied. The pH-dependent stability and the salt tolerance of MFs were different owing to the dissociation of the outermost hydrophilic groups and the hydrophobic interactions scaling with the alkyl chain length of surfactant. The hydrophobic interactions are favored only for oleic and myristic acid double layers. In these MFs, aggregation cannot be observed even in fairly dilute systems up to the physiological salt concentration around neutral pH 6–8 favored in biomedical application. The stable oleic and myristic acid double layers can hinder effectively the aggregation of magnetite particles due to the combined steric and electrostatic stabilization.

1. Introduction

In biocompatible MFs, iron oxide nanoparticles are coated with biocompatible molecules [1–4]. Fatty acids as surfactants are also used [4–6]. Surfactant double layers are able to stabilize magnetic nanoparticles in a water carrier. The formation of the first layer often involves chemical bonds on the active sites of the particle surface (e.g. Fe–OH on magnetite, 5–10 sites nm^{-2}) [7]. The second layer forms via hydrophobic interaction. Electrostatic, steric and combined stabilization layers can develop [8]. The thicker coating provides better stability, especially if magnetic field is applied [9].

The use of various fatty acids to prepare water based MFs from magnetite nanoparticles dates back to the early 1980s as read in the papers [10, 11], in which the ability of C6–C18 carboxylic acids to stabilize aqueous MFs was compared and the structure of formed double layers as well as the surface density of fatty acids (∼5–2.5 molecules nm^{-2}) were revealed. This well known term was called the grafting number in a recent paper [12], and so the packing density in the coating layers have been reinvented without classical adsorption measurements. Great efforts have been made to improve the quality of fatty acid double layer stabilized MFs and lots of papers have been published [13–19], mentioning here only some recent ones. The oleate coating on magnetite is favored, especially if the aim is to further functionalize the magnetic nanoparticles [20–24]. Structural characterization by SANS [17, 18] revealed the existence of large agglomerates in most of the water based MFs. Less attention was paid until now to the adsorption of fatty acids, the charge neutralization and overcharging due to the first and second layer formation. The effect of dilution, pH and salt concentration has also remained in the background, although these are the most important factors in biomedical application. In this work, we attempted to clear up some basic questions studying an oleate double layer stabilized magnetite in detail, and comparing

this with different chain length fatty acids to choose the most promising double layer stabilized MF for biomedical application.

2. Experimental details

2.1. Materials

The co-precipitation method was used to prepare superparamagnetic magnetite with particle size below 10 nm. Combinations of surfactants dodecyl-benzenesulfonic acid (DBSA), lauric (dodecanoic) acid (LA), myristic (tetradecanoic) acid (MA) and oleic (unsaturated octadecanoic) acid (OA) as well as sodium oleate (NaO) were used for coating magnetite nanoparticles in order to be dispersed in water. The quantity of surfactant added to 1 g of precipitate varied between 0.3 and 0.5 g. The details of MF preparation and the characterization of magnetite itself have been published [16, 19, 25–27].

All experiments were performed at room temperature (25 ± 1 °C). All reagents were of analytical grade product apart from the technical grade surfactants, and Milli-Q water was used.

2.2. Methods

2.2.1. Adsorption. The adsorption isotherm of Na oleate at pH ∼6.5 and 0.01 M NaCl was determined by the batch method. The magnetite suspensions (1 g l^{-1}) were equilibrated with the series of oleate solutions up to 3 mmol l^{-1} concentration in closed test tubes for 24 h, at room temperature. The equilibrium concentration of oleate was measured in the supernatants after perfect separation of magnetite by centrifuging at 13 000 RPM for 1 h and membrane filtration (0.22 μm).

2.2.2. Electrophoretic mobility—laser Doppler electrophoresis. Electrophoretic mobilities of the pure magnetite (0.05 g l^{-1}) samples and that with different oleate contents (0.002–0.15 mmol l^{-1}) were measured in the range of pH about 3–10 at 25 ± 0.1 °C in a disposable zeta cell (DTS 1060) of a NanoZS (Malvern, UK) apparatus. The zeta potential was calculated by the Smoluchowski equation [8].

2.2.3. Particle sizing—dynamic light scattering (DLS). The same apparatus operating in backscattering mode at angle 173° was used. Dilute systems (0.1 g l^{-1} magnetite, 0.01 M NaCl) were measured in the range of pH 3–10. The effect of oleate loading (0.02–0.2 mmol l^{-1}) was investigated. The Z average sizes calculated from third order cumulant fits of the measured correlation functions at a given kinetic stage (measured 50 s after the ultrasonication) are presented.

2.2.4. Coagulation kinetics followed by DLS. The salt tolerance of oleic acid double layer stabilized systems was tested by using a Zetasizer 4 (Malvern, UK) apparatus. The NaCl concentration was changed gradually from 0.01 to 0.4 M in the dilute sols (0.0125 g l^{-1}) at pH ∼6. The size evolution of aggregates was followed in time typically for an hour with a time resolution of 2 min.

3. Results and discussion

3.1. pH-dependent surface charging of magnetite

Magnetite is an amphoteric solid developing charges in the protonation ($\underline{Fe}$–OH + H^+ ⇔ $\underline{Fe}$–OH_2^+) and deprotonation ($\underline{Fe}$–OH ⇔ $\underline{Fe}$–O^- + H^+) reactions of $\underline{Fe}$–OH surface sites. It has a characteristic pH, the point of zero charge (PZC), where surface charge density is zero [28, 29]. The surface charging of magnetite used in this work has been characterized [27, 30]. Its PZC is at pH 7.9 ± 0.1 and so particles are positively charged below pH ∼8, while negatively above it. The net surface proton excess amounts varied from +0.3–0.1 mmol g^{-1} at pH ∼4 to −0.1–0.15 mmol g^{-1} at pH ∼10 in 1–0.01 M NaCl solutions, and hence the surface charge densities also ranged from +0.3–0.1 C m^{-2} at pH ∼4 to −0.1–0.15 C m^{-2} at pH ∼10 considering the specific surface area 95.3 m^2 g^{-1} [27]. These values show that less than 2$\underline{Fe}$–OH sites from the 5–10 nm^{-2} can become charged, in agreement with the literature [28, 29].

3.2. Adsorption of Na oleate on magnetite

We measured the oleate adsorption on magnetite as shown in figure 1 (left). The two step shape of the adsorption isotherm is characteristic of surfactant adsorption from aqueous solutions [31]. The first step, belonging to the monolayer formation, seems to be completed below ∼1 mmol g^{-1}, while the second step goes up to the saturation value, ∼2 mmol g^{-1}, indicating the completion of double layer formation. We performed a model calculation knowing the geometry, particle size (spherical, 6.7 ± 1.7 nm [27]) and solid density (5.18 g cm^{-3} [12]) of magnetite to support the measured data for mono and double layer formation. The amount of oleate coating on 1 g magnetite nanoparticles of size from 4 to 12 nm was calculated and plotted (figure 1 right) using two values of packing densities 0.38 and 0.2 nm^2 per oleate, expanded in the first and compressed in the second layer, respectively, as given in [10]. Taking the sum of oleate amounts belonging to the actual sizes (6.7 nm for the first and 8.7 nm for the second layer) gives 1.92 mmol g^{-1}, which accords well with the value of ∼2 mmol g^{-1} assigned to the double layer coverage. If the densely packed fatty acids (0.20–0.22 nm^2 per molecule) had been assumed in both layers as suggested [32], the calculated double layer coverage (>3 mmol g^{-1}) would not have been comparable with the measured value. The surface coverage, ∼1 (0.78) mmol g^{-1}, in the first layer is high above the density of positively charged sites, 0.05 mmol g^{-1}, at pH ∼6, 0.01 M NaCl [27], but in good agreement with the number of available ($\underline{Fe}$–OH) surface sites, 0.8 mmol g^{-1}, considering the $\underline{Fe}$–OH site density (5 sites nm^{-2}) and the specific surface area (95.3 m^2 g^{-1}). These facts support the complex formation between the –COOH groups of oleate and the $\underline{Fe}$–OH sites on magnetite, which has been assumed [10, 12, 20, 32]. This interaction is not Coulombic; the positive potential on magnetite surface at pH ∼6 only enhances the surface complex formation [30].

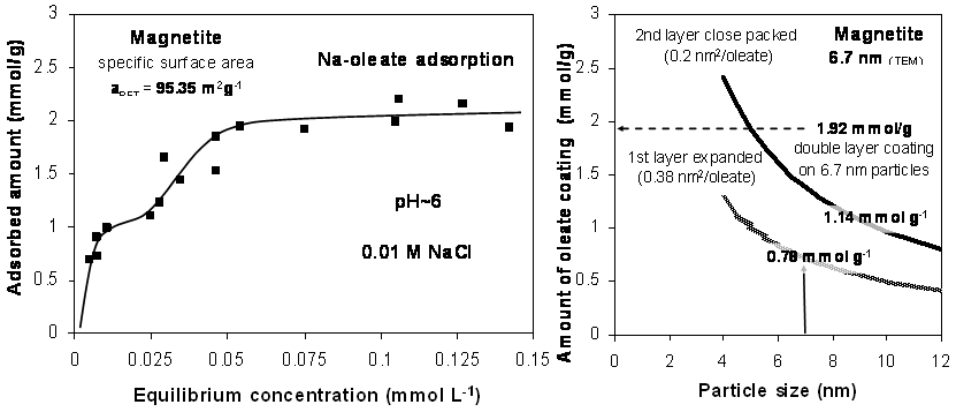

Figure 1. Adsorption isotherm measured at room temperature (left). Calculated amount of oleate coating on magnetite surface assuming loose and close packed layers (right).

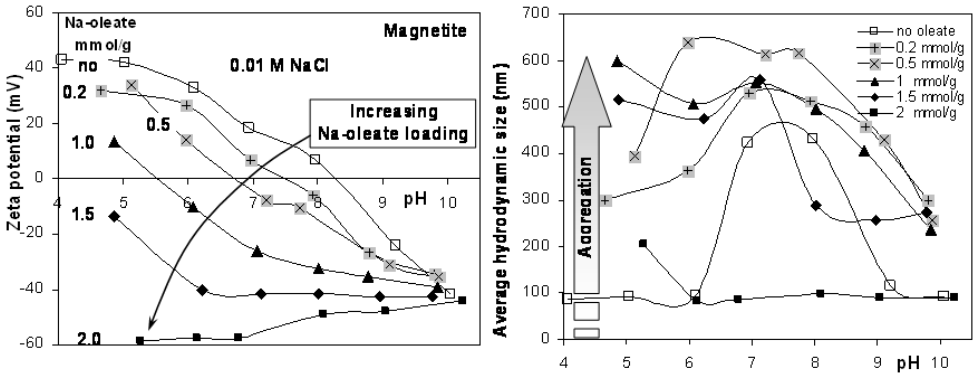

Figure 2. Effect of Na oleate loading on pH-dependent charge state (left) and aggregation (right) of magnetite in 0.01 M NaCl solutions at 25 ± 0.1 °C. (The reproducibility of the zeta potential was ±5 mV.)

3.3. The effect of oleate on magnetite particle charge

The influence of oleate addition on the charge state of magnetite particles was studied in parallel. The measured zeta potential data showed the dominance of positive charges on magnetite at pH ∼6 up to 0.04 mmol l^{-1} oleate concentration. However, above this concentration the sign of zeta potential reversed, indicating the sign reversal of the charges on magnetite surface occurring with increasing oleate loading. The specific oleate amount was ∼0.75 mmol g^{-1} at this charge neutralization point, in fairly good agreement with the oleate amount in the first layer from adsorption results. The positive magnetite particles (below the pH of PZC ∼8 [25]) became negative, i.e. anionic particles formed, due to the dissociated carboxylate groups (–COO–) oriented toward the aqueous medium in the second layer.

3.4. The effect of oleate loading on the pH-dependent charge state and aggregation of magnetite

The zeta potential measured in pure magnetite sols and in the presence of different oleate amounts over a broad range of pH can be seen in figure 2 (left). The amphoteric character of pure magnetite (open squares) is obvious. The zeta potential reversal occurs at pH ∼8, which may be identified as the isoelectric point (IEP) in agreement with PZC. The IEP of magnetite falls between 7 and 9 [7, 28].

The effect of oleate was examined at several concentrations; some of them are shown in figure 2 (left). It can be seen that zeta potential decreases gradually with increasing oleate loadings over the whole range of pH. The pH of zeta potential reversal shifts to lower pH values with increasing oleate addition. The zeta potential becomes negative even at low pHs above oleate loading ∼1.5 mmol g^{-1}. First, the oleate adsorbed in the first layer neutralizes the positive charges on the magnetite surface up to ∼1 mmol g^{-1}, in good harmony with the adsorption results (figure 1); then anionic particles form during the further adsorption, if there are enough oleate ions present to build up the second layer on the nanoparticles. Due to the close packed structure of oleate anions in the second layer, the measured values become more negative than for naked magnetite in the alkaline pH region.

In parallel, the pH-dependent particle aggregation was measured by DLS, which can be used even in a coagulating system [33]. In the pure magnetite sols, only the electric double layer exists far from the PZC, which is able to stabilize particles at low salt concentration, so the measured sizes remained below 100 nm (figure 2 right, open squares). However, in the absence of electrostatic stabilization near the pH of PZC, large aggregates form even at low (0.01 M)

salt concentration. Only large aggregates could be measured from the lowest oleate loading up to the completion of double layer formation over the whole range of pH studied. When stabilized, double layer coated anionic particles are dispersed at the oleate loading of 2 mmol g^{-1}; reproducible size values smaller than ∼100 nm were measured independently of the pH above pH ∼6. The outermost hydrophilic shell on the double layer coated magnetite particles contains carboxylate groups. Therefore, pH-dependent negative charges exist due to the dissociation of bound groups, –COOH ⇔ $–COO^- + H^+$ (pK ∼4). Fully dissociated carboxylate groups above pH ∼6 provide electrostatic repulsion between colliding particles besides the steric hindrance of the double layer. However, the dissociation degree starts to decrease with decreasing pH below pH ∼6, and so not only does the electrostatic repulsion decline, but also particles become less hydrophilic in the acidic region.

3.5. Colloidal stability of dilute magnetic fluids: pH dependence and salt tolerance

Combinations of anionic surfactants (DBSA + DBSA, LA + LA, MA + MA, OA + OA, LA + DBSA, MA+DBSA) were used. DBSA stabilized MF samples are not biocompatible and were considered here for comparative investigations. The details of stabilization/dispersion of magnetite nanoparticles in water carrier to obtain stable magnetic fluids depend on the surfactant combination [16, 19]. The quantity of surfactant added to 1 g of freshly prepared magnetite varied between 0.3 and 0.5 g. Considering the molecular weights of compounds in question, the specific amount of surfactants ranges over 1.5–2 mmol g^{-1} in high quality water based magnetic fluids. This range accords well with the results of oleate adsorption, where the double layer formation was proved, and the adsorbed amount, 2 mmol g^{-1}, was assigned to the completion of the second layer coverage as discussed above.

Several properties (magnetic saturation, SANS, etc) of these concentrated MFs have been studied and published in the last few years [15–19]. The sizes of primary particles seemed to be similar (magnetic size 4.9–6.8 nm); the influence of surfactant type was not so evident. However, the effect of dilution, pH and salt concentration has not been investigated yet. Besides an attempt at the direct sizing of dense MFs (table 1) with a NanoZS apparatus working in backscattering mode, we characterized the pH-dependent stability and salt tolerance of these MFs in dilute aqueous systems.

The direct DLS measurement of original, dense magnetic fluid samples was possible to execute; however, the quality of correlation functions was not good enough, as shown by high polydispersity indices (PDIs) in the second column of table 1. Therefore, the calculated sizes cannot be considered as real values. The size data from DLS measurements have to be interpreted cautiously, even those measured under optimal conditions as collected in table 1 for diluted systems. These values seem to be too large related to the size data from magnetization measurements, where the primary particle sizes were 4.9–6.8 nm [16], or those from small angle neutron scattering (SANS), detecting 10–20 nm primary aggregates besides the formation of large (>100 nm in size) fractal aggregates, being out of the observation scale of the SANS device [17, 18], even though we know that DLS measures hydrodynamic size. The size data in the table 1 are *Z* average hydrodynamic sizes calculated from the intensity distribution functions as the direct, least manipulated source in DLS evaluation.

Table 1. Average size values in magnetic fluids determined by DLS at 25 ± 0.1 °C in the concentrated MFs (direct) and dilute systems at pH ∼7. (*Z* average sizes calculated from intensity distribution.)

Sample	Direct[a] (PDI) size (nm)	Diluted by water size (nm)	in 0.15 M NaCl[b] size (nm)
DBSA + DBSA	47 (0.372)	270	165
LA + DBSA	111 (0.439)	64	>1000
MA + DBSA	102 (0.625)	33	152
LA + LA	185 (0.375)	77	>1000
MA + MA	78 (0.330)	48	51
OA + OA	132 (0.375)	37	99

[a] The polydispersity indices (PDIs) are too high to accept the values as real.

[b] Diluted by physiological salt solution, pH ∼6.5, and measured after 1 h.

To illustrate the different evaluation possibilities in the DLS method the number and intensity distribution functions of the dilute OA + OA and LA + LA MFs are compared in figure 3. Considering the more intensive light scattering of larger particles over the colloidal size range [8], the larger aggregates weight the intensity distribution even if their amounts are not dominant. On the other hand, these cannot affect the number distribution functions at all, such as shown in figure 3, if their amount is not significant related to the smaller particles. Therefore, the calculable number average sizes in the oleic and lauric acid double layer stabilized magnetic fluids are fairly small, 14 and 20 nm, respectively, and more these agreed well with the sizes from SANS studies [17, 18].

The double DBSA layer stabilized MF was strongly aggregated; the average size of hydrodynamic units varied between 160 and 270 nm depending on the pH from 3.4 to 7 and the salt concentration up to 0.15 M NaCl. The combined layers of DBSA with LA and MA resulted in larger (∼64 nm at pH ∼6.2) and smaller (∼33 nm at pH ∼6.3) aggregates, respectively, in accordance with SANS results [17]. However, any change in solution conditions such as adjusting pH to 7 and adding salt to MFs unexpectedly induced a fast aggregation. So the DBSA and its combined applications with LA or MA seem to be not sufficient in water based MF stabilization. The best stabilization was reached with the MA and OA double layers (table 1).

The effect of pH and salt on the stability of dilute samples of LA, MA and OA double layer stabilized MFs was studied analogously to the oleate coated samples. The electrophoretic mobility and the average size in a given kinetic stage were measured at pHs 3–9 and plotted in figure 4.

For the sake of comparison the data measured for the naked magnetite are also given as a function of pH. It can be seen that the sign of electrophoretic mobilities is negative for all samples of the diluted MFs in the whole pH region (figure 4

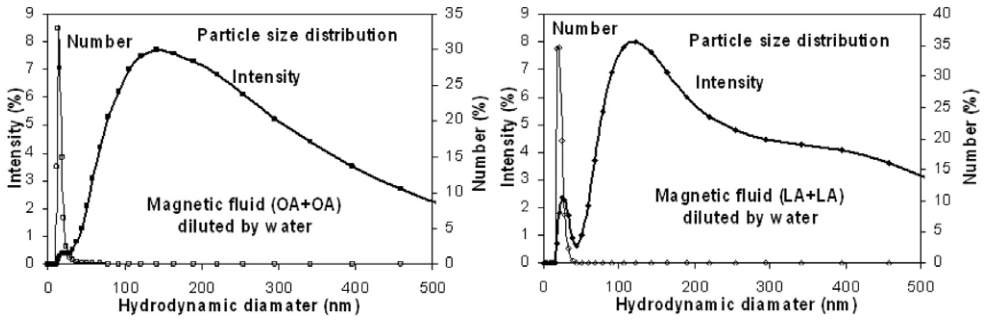

Figure 3. Comparison of the number and intensity distribution functions calculated from the same DLS data set. Results for the dilute oleic (OA + OA) and lauric (LA + LA) acid stabilized samples are shown on the left- and right-hand sides, respectively.

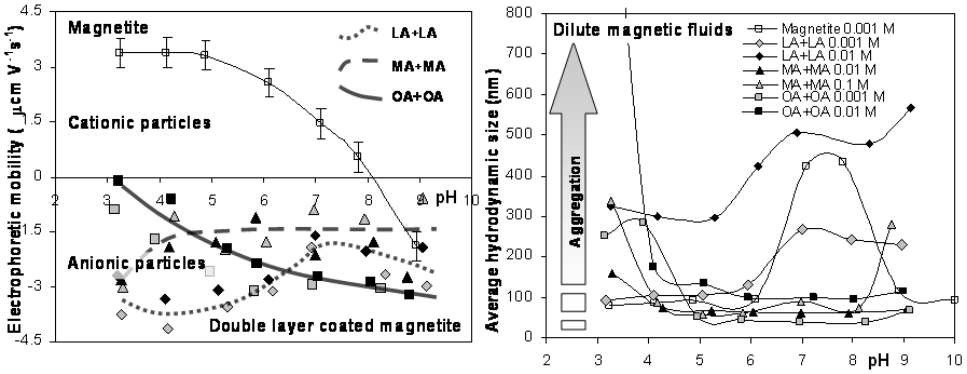

Figure 4. Effect of anionic surfactant double layer coating on the pH-dependent charge state (left) and aggregation (right) of magnetite particles in 0.001, 0.01 and 0.1 M NaCl solutions at 25 °C.

left), so all the particles are anionic, proving the presence of a double layer coating uniformly. However, the change in the mobility values with increasing pH is characteristically different depending on the alkyl chain length of the fatty acids studied here. The oleic acid has the longest chain (n_C is 17) among the samples, and the negative mobility values of OA + OA stabilized particles increase monotonically with increasing pH, i.e., the particles hold more and more charges due to the advancing dissociation of –COOH groups forming $–COO^-$ charges in the outermost layer of particles. In parallel, aggregation does not occur in the OA + OA samples above pH ∼5 (figure 4 right), when particles hold charges and become hydrophilic. In contrast with this, the sample stabilized with lauric acid, having the shortest chain (n_C is 11) here, shows practically the opposite trend. The greatest negative mobility values were measured at pHs between 3 and 5, then a significant decrease was experienced up to pH ∼ 7, which shows a decrease in negative charges carried by lauric acid double coated particles without doubt. To understand this seemingly contradictory behavior, we have to consider the effect of alkyl chains, i.e. the hydrophobic interactions. The simple fact is that the shorter the chain the greater the affinity of surfactant for water, so making it less favorable for it to remain in the adsorption layer [10]. The salts of lower molecular weight fatty acids like Na laurate formed here with increasing pH are increasingly water soluble and are hence liberated from the adsorption layer. In the case of the LA + LA double layer, the hydrophobic interactions are not effective enough to maintain the close packed second layer in the neutral and slightly alkaline region. The particle aggregation in the LA + LA samples starts above pH ∼6 (figure 4 right) in accordance with the declining structure of the stabilizing double layer. The behavior of myristic acid (n_C is 13) stabilized particles is just between those explained above. The electrophoretic mobilities do not change practically from pH ∼4 to 9 (figure 4 left), and although their low values cannot point to a high surface charge density the stability of the MA + MA coated particles was the best (figure 4 right), fortunately in the pH region between 5 and 8, which biomedical application focuses on.

The salt tolerance of the oleic acid double layer stabilized magnetic nanofluids was investigated in dilute systems at pH ∼6. We should note that the salt tolerance of naked magnetite particles is very low (∼0.001 M NaCl) under this condition. Coagulation kinetics measurements were performed to determine quantitatively the stabilization effect as explained before [8, 25]. The stability ratio (W) was calculated as suggested [33] and the stability limit 0.2 M NaCl was obtained from the $\log_{10} W$ versus electrolyte concentration function. Therefore, the oleate double layers can hinder effectively the aggregation of magnetite particles due to the combined steric and electrostatic stabilization, and the resistance against electrolytes is enhanced above the critical salt tolerance (>0.150 M) expected under physiological conditions.

4. Conclusion

We answered some basic questions such as the adsorption of oleate/oleic acid as an example among fatty acids, the double layer formation, the charge neutralization and overcharging due to the first and second layer formation on magnetite nanoparticles in water based systems. The most important part of this work is that the effect of dilution, pH and salt concentration on the MFs stabilized by a series of different surfactant combinations has been revealed, which are the most important factors in biomedical application. Comparing the MFs with different chain length fatty acids, only the OA + OA and MA + MA double layer stabilized magnetic fluids were able to be dispersed well with dilution; aggregation could not be observed even in fairly dilute systems up to the physiological salt concentration in the pH region favored in living systems.

Acknowledgments

This work was supported by the grants OMFB-01604/2006 and NKTH-OTKA (A7-69109/2007), as well by the Romanian CEEX research projects MAGMED and NANOFUNC.

References

[1] Pankhurst Q A, Connolly J, Jones S K and Dobson J 2003 *J. Phys. D: Appl. Phys.* **36** R167–81
[2] Bahadur D and Giri J 2003 *Sadhana* **28** 639–56
[3] Saiyed Z M, Telang S D and Ramchand C N 2003 *BioMagn. Res. Technol.* **1** 2
[4] Gupta A K and Gupta M 2005 *Biomaterials* **26** 3995–4021
[5] Rosensweig R E 1985 *Ferrohydrodynamics* (Cambridge: Cambridge University Press)
[6] Scherer C and Figueiredo Neto A M 2005 *Braz. J. Phys.* **35** 718–27
[7] Cornell R M and Schwertmann U 1996 *The Iron Oxides* (Weimheim: VCH)
[8] Hunter R J 1987 *Foundations of Colloid Science* vol 1 (Oxford: Clarendon)
[9] Odenbach S 2003 *Colloids Surf.* A **217** 171–8
[10] Wooding A, Kilner M and Lambrick D B 1991 *J. Colloid Interface Sci.* **144** 236–42
[11] Wooding A, Kilner M and Lambrick D B 1992 *J. Colloid Interface Sci.* **149** 98–104
[12] Chen K, Bakuzis A F and Luo W 2006 *Appl. Surf. Sci.* **252** 6379–82
[13] Urban P, Idzikowski B, Kostyrya S, Andrzejewski B and Vértesy Z 2004 *Czech. J. Phys.* **54** D683–6
[14] Kikura H, Matsushita J, Matsuzaki M, Kobayashi Y and Aritomi M 2004 *Sci. Technol. Adv. Mater.* **5** 703–7
[15] Vékás L, Bica D, Marinica O, Raac M, Socoliuc V and Stoian F D 2005 *J. Magn. Magn. Mater.* **289** 50–3
[16] Vékás L, Bica D and Marinica O 2006 *Rom. Rep. Phys.* **58** 217–28
[17] Avdeev M V, Aksenov V L, Balasoiu M, Garamus V M, Schreyer A, Török Gy, Rosta L, Bica D and Vékás L 2006 *J. Colloid Interface Sci.* **295** 100–7
[18] Balasoiu M, Avdeev M V, Aksenov V L, Hasegan D, Garamus V M, Schreyer A, Bica D and Vékás L 2006 *J. Magn. Magn. Mater* **300** e225–8
[19] Bica D, Vékás L, Avdeev M V, Marinica O, Balasoiu M and Garamus V M 2007 *J. Magn. Magn. Mater.* **311** 17–21
[20] Hong R Y, Zhang S Z, Han Y P, Li H Z, Ding J and Zheng Y 2006 *Powder Technol.* **170** 1–11
[21] Park S I, Kim J H, Kim C G and Kim C O 2007 *J. Magn. Magn. Mater.* **312** 386–9
[22] Józefczak A, Skumiel A and Łabowski M 2005 *J. Magn. Magn. Mater.* **290/291** 265–8
[23] Lattuada M and Hatton T A 2007 *Langmuir* **23** 2158–68
[24] Morais P C, Santos J G, Neto K S, Pelegrini F and De Cuyper M 2005 *J. Magn. Magn. Mater.* **293** 526–31
[25] Illés E and Tombácz E 2006 *J. Colloid Interface Sci.* **295** 115–23
[26] Tombácz E, Libor Zs, Illés E, Majzik A and Klumpp E 2004 *Org. Geochem.* **35** 257–67
[27] Tombácz E, Illés E, Majzik A, Hajdú A, Rideg N and Szekeres M 2007 *Croat. Chem. Acta* **80** 503–15
[28] Kosmulski M 2001 *Chemical Properties of Material Surfaces* (New York: Dekker) p 753
[29] Sun Z, Su F, Forsling W and Samskog P 1998 *J. Colloid Interface Sci.* **197** 151–9
[30] Illés E and Tombácz E 2003 *Colloids Surf.* A **230** 99–109
[31] Giles C H, Smith D and Huitson A 1974 *J. Colloid Interface Sci.* **47** 755–65
[32] Shen L, Laibinis P E and Hatton T A 1999 *Langmuir* **15** 447–53
[33] Schudel M, Behrens S H, Holthoff H, Kretzschmar R and Borkovec M 1997 *J. Colloid Interface Sci.* **196** 241–53